SCIENCE CHINA
Technological Sciences

•Article•

https://doi.org/10.1007/s11431-019-1591-7

Aligned Ni nanowires towards highly stretchable electrode

LI JiDong*, NIU JiYuan, LI XueMei, ZHOU JianXin, HU ZhiLi & GUO WanLin*

State Key Laboratory of Mechanics and Control of Mechanical Structures, The Key Laboratory of Intelligent Nano Materials and Devices of DoE, Institute of Nano Science of Nanjing University of Aeronautics and Astronautics, Nanjing 210016, China

Received December 18, 2019; accepted April 8, 2020; published online May 29, 2020

Easy fabrication of super-stretchable electrodes can pave the way for smart and wearable electronics. Using drop casting unidirectional nickel nanowires with polyurethane matrix, we fabricated a super-stretchable film with high electric conductivity. The as-fabricated film can withstand a 300% tensile strain in the direction perpendicular to nanowires, owing to the transformation of percolating nanowire network from 2D to 3D. In contrast to the decreased film conductivities under large tension in most stretchable electrodes, which usually associate with fractures and irreversible deformations, our film conductivity can increase with the applied strain. This probably benefits from the enhanced electrical contacts between twisted nanowires under tension. The developed super-stretchable film with unprecedented behavior in this work sheds light on the facile fabrication of super-stretchable electrodes with durable performance.

nickel nanowire, stretchable electrode, polyurethane matrix, three-dimensional network, alignment

Citation: Li J D, Niu J Y, Li X M, et al. Aligned Ni nanowires towards highly stretchable electrode. Sci China Tech Sci, 2020, 63, https://doi.org/10.1007/s11431-019-1591-7

1 Introduction

Flexible and stretchable devices have attracted extensive interest due to the expanding demands for wearable electronics, artificial skin and muscles [1–5]. Inevitably, reliable electrodes that can retain good conductivity during stretching are highly desired to effectively power or electrically interconnect the systems [6,7].

There are two prominent strategies to achieve stretchable electrodes: conductive elastomers and conductive structures that can stretch. Regarding the former strategy, it has been well known for decades to give rubber conductivity by filling and dispersing carbon black [8,9]. Similar doping method has been extensively used to acquire intrinsically conductive elastomers. However, they probably suffer from considerable resistance change and poor conductivity during stretching, which limit their application as electrodes [10–12].

As to the conductive structure strategy, it integrates recoverable elastomers with highly conductive film or wires that are delicately designed into stretchable structures. Wavy geometry, coiled spring, buckling and serpentine configuration have been developed for metal film to stretch [13–17]. In spite of good conductivity, they commonly fail under very large strains over 100% due to the rigidity of the metal film. Combining robust structures with emerging nanomaterials such as metal nanowires [18], carbon nanotubes (CNT) and graphene shed new light on super-stretchable conductive electrodes. Advanced structures e.g. forest and bridged layers are specially designed to further enhance the function of CNT and grapheme [19,20]. Two-dimensional (2D) percolating networks based on silver nanowires can even exhibit good conductivity under 300% strains [21]. However, almost all these super-stretchable structures show bad performance with large deformations due to the formation of cracks or the loss of effective contact junctions.

Here, we explore a mutually twisting three-dimensional (3D) structure that could be stretched over 300% and possess

*Corresponding authors (email: j.d.li@nuaa.edu.cn; wlguo@nuaa.edu.cn)

even higher conductivity under such large strain. To achieve this robust structure, nickel nanowires (NiNWs) are aligned by the magnetic field in the same direction and then processed with the polyurethane (PU) to a membrane. A 2D percolating Ni network forms in the hybrid membrane. Further treating the samples with large strains perpendicular to the alignment direction, the 2D structure can develop into a twisted 3D network that are super-stretchable and conductive. This strain-induced 3D percolating structure has even better conductivity under large tension due to the enhanced contact of the twisted junctions among the nanowires during stretching.

2 Method

2.1 Ni nanowires growth

The magnetic-field assisted aqueous solution method has been successfully employed to produce high aspect ratio NiNWs. Their typical size is around 500 nanometers in diameter and several hundreds of micrometers in length as shown in Figure S1(a) and (b). Our preparation process is based on previous works [22,23]. Firstly, 50 mL aqueous solution containing 0.1 M nickel chloride hexahydrate ($NiCl_2{\cdot}6H_2O$), 37.5 mM trisodium citrate dihydrate ($Na_3C_6H_5O_7{\cdot}2H_2O$) and 0.2 mM chloroplatinic acid hexahydrate ($H_2PtCl_6{\cdot}6H_2O$) were prepared. Its pH value is measured by a pH meter and adjusted to 13.8 by 5 M sodium hydroxide (NaOH). Another 50 mL aqueous solution containing 10% hydrazine hydrate ($N_2H_4{\cdot}6H_2O$) was prepared. Both the solutions were warmed up to 80°C and then mixed in a beaker. The beaker was then placed in an 80°C water bath and sandwiched between two neodymium magnets that could provide a magnetic field over 0.2 T for the growth solution. After a 10–20 min reaction, the NiNWs grew and aggregated into black fluffy mass at the surface and bottom of the aqueous solution. Placing a magnet outside the beaker bottom could rapidly precipitate the black products and keep them stick on the bottom wall when pouring out the solution. In this way, we washed the NiNWs by deionized water and ethanol for several times. Finally, the as-prepared NiNWs were stored in the ethanol in the concentration of 1–5 mg/mL for further application.

2.2 Preparation of NiNWs/PU composites

The NiNWs/PU membranes were produced in three steps utilizing a conventional drop-casting method with our NiNWs alignment technique as illustrated in Figure 1(a). In the first step, the as-prepared NiNWs in ethanol were stirred to disperse well and then uniformly dropped at the glass surface. During the drop-casting process, two face-to-face magnets provided a quasi-parallel magnetic field to align these NiNWs in the roughly same direction. After a compact and uniform NiNWs layer was deposited, it was dried in a vacuum. We repeated the previous step to increase the NiNWs layer thickness if necessary. An aligned NiNWs film was thus prepared on the glass as shown in Figure S1(c) and (d). Next, a layer of PU solution was dropped on the NiNWs layer and then dried in the fume hood. The PU solution was prepared in Tetrahydrofuran (THF) in the mass ratio of 1:10. Finally, a black and elastic membrane could be easily peeled off from the glass as shown in Figure 1(b).

2.3 Characterization

The scanning electron microscopy (Zeiss, EVO 18) was performed at 10 kV acceleration voltage to observe the morphology of the hybrid membrane. The motorized linear stage (Lyseiki, ZP150-50H) was employed to do tensile tests with 3 μm positional resolution. During the test, Keithley 2400 SourceMeter was recording the resistance change in real-time.

3 Results and discussion

Scanning electron microscope (SEM) images shown in Figure 1(c) and (d) display the hybrid structure of the membrane consisting of a ~50 μm thick NiNWs layer and a ~100 μm thick PU layer. The NiNWs are well integrated into a compact layer by the infiltrated PU, which shows a single-oriented texture due to the magnetic-field-assisted alignment during the membrane fabrication.

Although the NiNWs layers are supposed to be rigid considering their large thickness compared with previous 2D percolating networks, it is surprising to find that the films can endure strain up to 300% and have an even better conductivity at such large deformation [21,24]. As shown in Figure 2(a)–(c), the black NiNWs/PU film is very flexible. It can be easily stretched and twisted in a large range. We use it as a flexible conductor to electrically connect the LED circuit as shown in Figure 2(d) and (e). Even though the hybrid film became deformed, it could rarely affect the electrical connection and the LED brightness. In order to investigate the electrical properties, we conducted tensile test to a stretchable film (Figure 2(f)). Its initial sheet resistance is around 800 Ω/sq. In the first loading cycle, the resistance falls by nearly a half at the 200%–300% strain. However, after unloading, it cannot recover to its original length and conductivity. The film is extended by 30%. The severe length extension indicates large structural transformation in the hybrid film. Nevertheless, in the second loading cycle with strains over 300%, the film showed much better reversibility. Its length recovers over 90% after releasing. The abnormal resistance drop is also observed when stretching the film. We

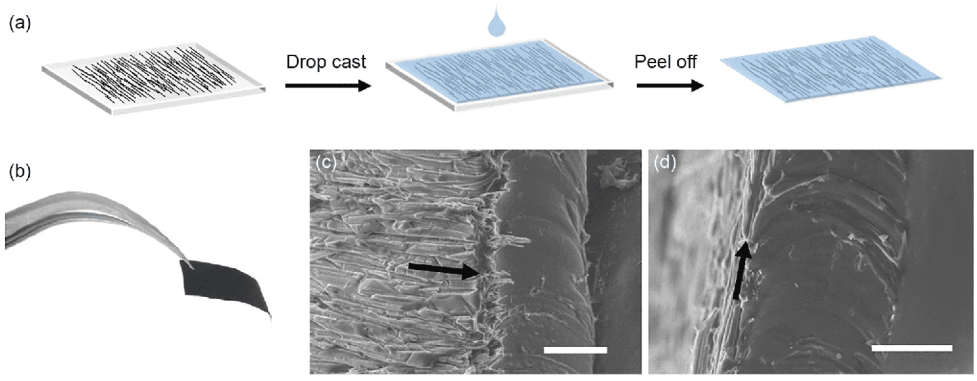

Figure 1 (Color online) (a) Schematic illustration of the fabrication procedure of NiNWs/PU membranes; (b) image showing a prepared membrane clamped by tweezers; (c,d) SEM images of the membrane top view (c) and cross-section view (d). The scalar bars are 40 μm and the black arrows illustrate the NiNWs alignment direction.

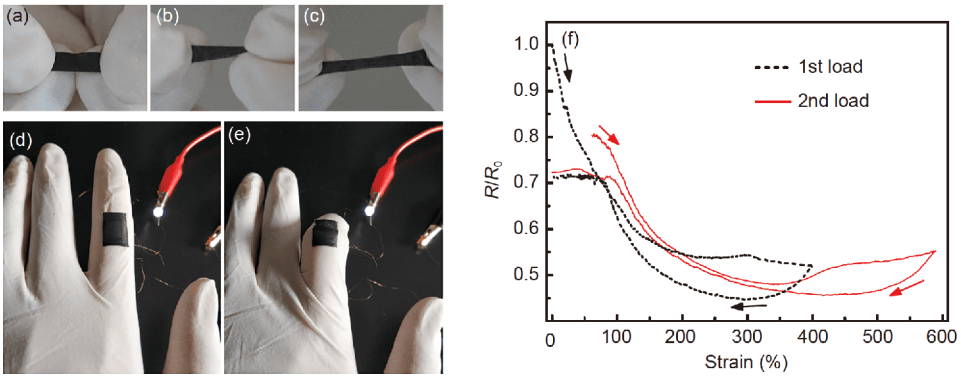

Figure 2 (Color online) (a)–(c) Images of the relaxed (a), twisted (b) and stretched (c) film; (d,e) photograph of an LED circuit connected by an as-prepared film as flexible electrode; (f) response of the relative resistance under large deformation. The original resistance R_0 is ~80 Ω.

noticed that after the turning point of the loading strain, the resistance would keep on decreasing to the minimum and then increase.

To elucidate the transformation mechanism of the NiNWs/PU membrane under large strain, we used SEM to see the morphology change of the film during uniaxial stretching as shown in Figure 3. The original state of the film before stretching is shown in Figure 3(a) and (e). The straight NiNWs bundles are densely buried in the PU layer and lead to parallel texture at the film surface. When stretching the film perpendicular to the NiNWs alignment direction with 200% in-plane strain, the straight NiNWs bundles are split apart and distorted into wave lines as shown in Figure 3(f). It is also interesting to find that the NiNWs layer becomes much thicker and develops a porous cross-link structure out of the plane (Figure 3(b)). When releasing the strain from 200% to 100%, the porous structure is compressed and the NiNWs realign into parallel structure (Figure 3(c) and (g)). In particular, the out of plane extrusion of the NiNWs layer is irreversible after the film is released (Figure 3(d)).

The ideal parallel array of NiNWs fails to explain the emerged structure out of the plane under the large in-plane strain. NiNWs aggregate together and form bundles with the percolating of PU. Actually, they probably intertwine as schematically depicted in Figure 4. During the uniaxial stretching, NiNWs are compelled to separate from each other to adapt the deformation. However, the entanglement of NiNWs will keep them together at the twisting point and thus transform the original compact structure into a cross-linked structure. It leads to a wavy network in the plane (Figure 4(b)) and dramatically increased thickness and porosity out of the plane (Figure 3(b)). After the unloading of strain, wavy wires in the porous structure are compressed into parallel states both in and out of the plane. The surface morphology recovers to the original parallel order (Figure 3(h)) while the sectional topography endures unrecoverable change and presents a new parallel order (Figure 3(d)). With simple stretching treatment, the NiNWs membranes could transform permanently from a 2D parallel network into a 3D alignment network that can achieve higher stretchability.

It should be noticed that the resistance of the hybrid membrane continually decreases during the stretching process until reaching ~200% strain (Figure 2(f)). The NiNWs network forms the conductive paths in the membrane. Its

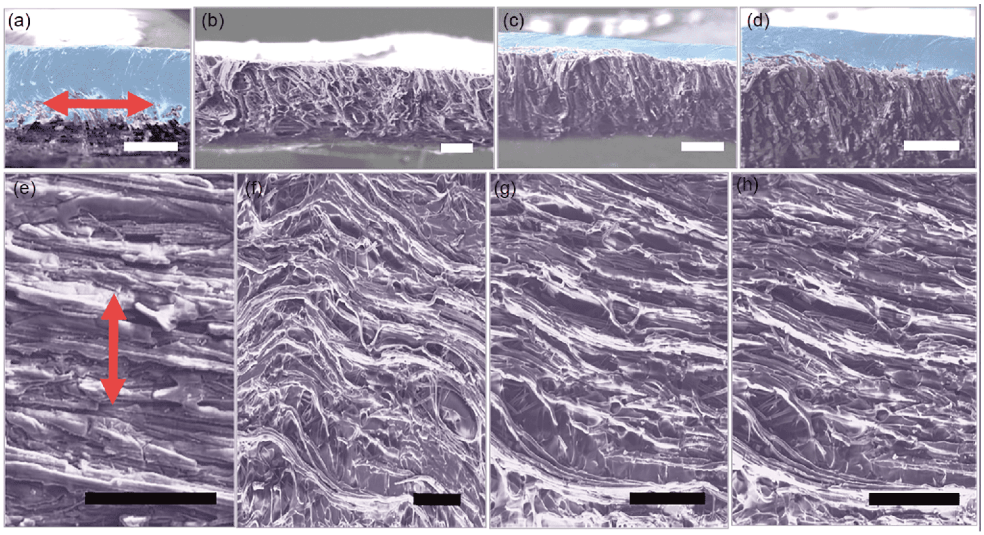

Figure 3 (Color online) False colored SEM images of the hybrid film under different strains with cross-section views (a)–(d) and top views (e)–(h) of the NiNWs/PU membranes under 0% (a,e), 200% (b,f), 100% (c,g) and 35% (d,h) strains. The red arrows in (a) and (e) illustrate the tensile direction. Scalar bars are 80 μm.

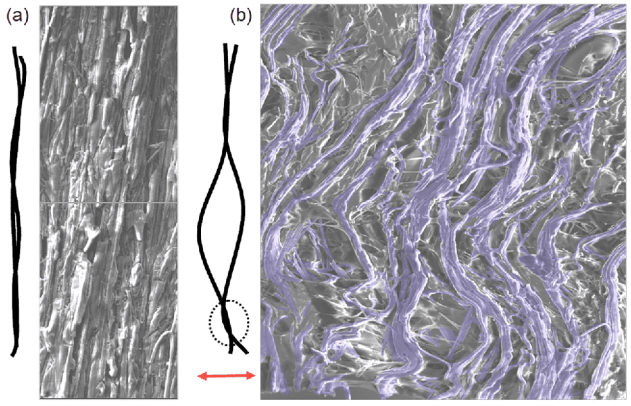

Figure 4 (Color online) SEM images of the surface NiNWs network in the relaxed state (a) and tensile state (b) with corresponding schematics on the left. The red arrow and dashed circle in (b) mark the stretching direction and twist junction, respectively.

resistance originates from two parts: the intrinsic resistance of nanowires and the contact resistance between nanowires. Considering the metal nature of nickel, the strain-induced resistance change of nanowires is ignored here. The contact resistance is predominantly from the tunneling effect. It should be quite sensitive to the tunneling distance and contact area. Normally, as large strain imposes, the structure becomes sparser, causing dramatic increase of tunneling distances and reducing of the contact areas, and thereby increase the resistance of the network. However, besides "normal" contacting junctions, NiNWs structure in our work also has many entangled nanowires. The mutual traction among the wires results in even tighter junctions where wires are inter-twisted and hence decreased tunneling distances. This accounts for the abnormal increase in the film's conductivity during stretching (Figure 2(f)). However, there is a competition between the improved contact at twist junctions and weakened contact at normal junctions.

The hybrid film is demonstrated to inherit both the hyperelasticity and good conductivity from PU and NiNWs, respectively. To explore their conductivity response when stretching, we conducted uniaxial tensile test for hundreds of cycles under different strains with the tensile direction perpendicular to the alignment direction as shown in Figure 5 (a). With small strains, they exhibit good stability. Under a 1% strain wave, their resistance changes less than 0.5% even after 500 cycles. For 2% strain cycles, however, the relative resistance would rapidly increase to 1.03 in the first 100 cycles and then gradually climb up to 1.05 in the following 400 cycles. Its conductivity tends to be stable after hundreds of cycles. Similar behavior appears in other super-stretchable composites based on Ag or CNT [24,25]. Cyclic strains of 50%–100% are also performed on a film as shown in Figure 5(c) and (d). The relative resistance of the film increases from 0.6 to 2.0 after 400 cycles. After long-term cyclic loading, the PU may intrinsically suffer irreversible deformation. The corresponding real-time response of the last 50 loading cycles when loading 2% strain cycles is shown in Figure 5(b). The resistance variation follows the triangular shape of the loading waves. To illustrate the dynamic loading response of the membrane more clearly, we applied both triangle and square loading waves and extracted several typical response cycles (Figure S2). Basically, the resistance response follows the tensile wave shape despite shoulder peaks are observed at the rising edge and falling edge of the strain load where the tensile rates suddenly change. The abrupt change of the strain rate during tensile tests may result in the apparent nonlinear rising of the resistance. We contribute these abrupt

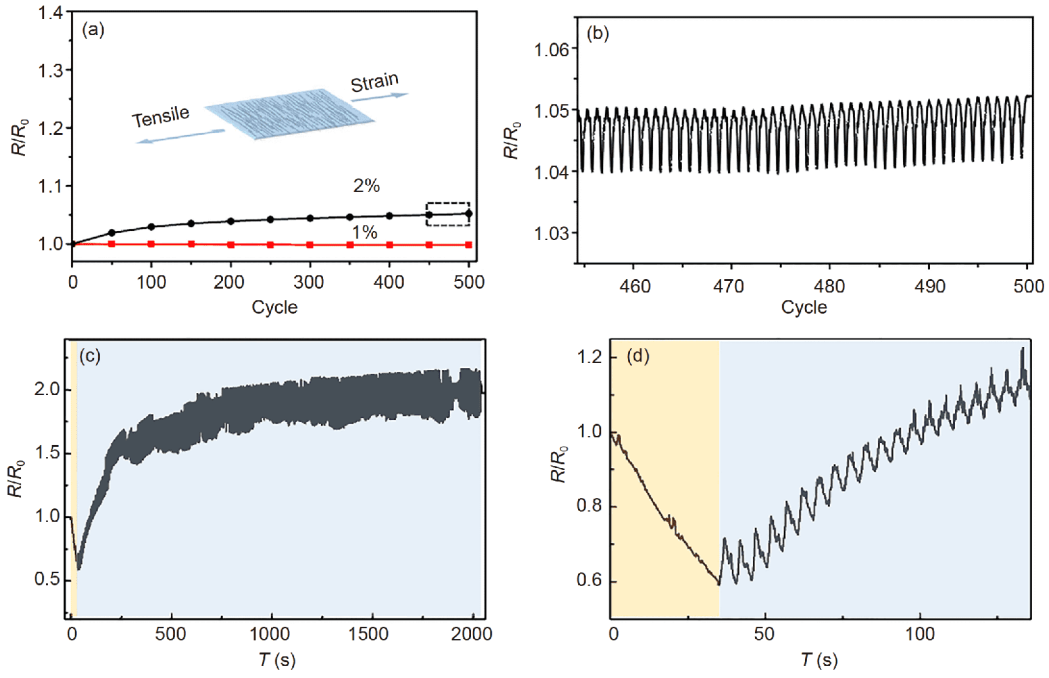

Figure 5 (Color online) Response of the relative resistance under strain cycles. (a) The resistance stability in 500 cycles tensile test. The schematic inset shows the tensile direction is perpendicular to the NiNWs alignment orientation. The dashed rectangle marks the last 50 cycles under 2% strain load in (b); (c, d) The film is stretched to 100% strain (the yellow section) and then endures cyclic strain of 50%–100% (the blue section). There are 400 cycles in (c) and the first 20 cycles are shown in (d).

changes in resistance to the viscoelastic PU, whose mechanical properties should be sensitive to the strain rate.

4 Conclusions

In summary, we developed a super-stretchable electrode structure that can exhibit increased conductivity at large deformation. Using unidirectional aligned NiNWs, the conventional 2D percolating networks inside the structure will be transformed into 3D twisted networks by tensile loads. It solved the problem of resistance increase that emerges when stretching most super-elastic electrodes and provided a novel strategy for the structural design of flexible and stretchable devices.

This work was supported by the National Key Research and Development Program of China (Grant No. 2019YFA0705400), National Natural Science Foundation of China (Grant Nos. 51535005, 51472117, 51702159), the Research Fund of State Key Laboratory of Mechanics and Control of Mechanical Structures (Grant Nos. MCMS-I-0418K01, MCMS-I-0419K01), the Fundamental Research Funds for the Central Universities (Grant Nos. NC2018001, NP2019301, NJ2019002), Natural Science Foundation of Jiangsu Province (Grant Nos. BK20170791, BK20180416), National and Jiangsu Postdoctoral Research Funds (Grant Nos. 2017M610328, 2018T110494 and 1701141B), and A Project Funded by the Priority Academic Program Development of Jiangsu Higher Education Institutions.

Supporting Information

The supporting information is available online at tech.scichina.com and link.springer.com. The supporting materials are published as submitted, without typesetting or editing. The responsibility for scientific accuracy and content remains entirely with the authors.

1 Bao Z, Chen X. Flexible and stretchable devices. Adv Mater, 2016, 28: 4177–4179
2 Lei Z, Wang Q, Sun S, et al. A bioinspired mineral hydrogel as a self-healable, mechanically adaptable ionic skin for highly sensitive pressure sensing. Adv Mater, 2017, 29: 1700321
3 Mirvakili S M, Hunter I W. Artificial muscles: Mechanisms, applications, and challenges. Adv Mater, 2018, 30: 1704407
4 Wen Z, Yeh M H, Guo H, et al. Self-powered textile for wearable electronics by hybridizing fiber-shaped nanogenerators, solar cells, and supercapacitors. Sci Adv, 2016, 2: e1600097
5 Chortos A, Liu J, Bao Z. Pursuing prosthetic electronic skin. Nat Mater, 2016, 15: 937–950
6 Lee H, Kim I, Kim M, et al. Moving beyond flexible to stretchable conductive electrodes using metal nanowires and graphenes. Nanoscale, 2016, 8: 1789–1822
7 Cheng T, Zhang Y, Lai W Y, et al. Stretchable thin-film electrodes for flexible electronics with high deformability and stretchability. Adv Mater, 2015, 27: 3349–3376
8 Medalia A I. Electrical conduction in carbon black composites. Rubber Chem Tech, 1986, 59: 432–454
9 Polley M H, Boonstra B B S T. Carbon blacks for highly conductive rubber. Rubber Chem Tech, 1957, 30: 170–179
10 Noh J S. Conductive elastomers for stretchable electronics, sensors and energy harvesters. Polymers, 2016, 8: 123
11 Park M, Park J, Jeong U. Design of conductive composite elastomers for stretchable electronics. Nano Today, 2014, 9: 244–260
12 Yang H, Yao X F, Zheng Z, et al. Highly sensitive and stretchable graphene-silicone rubber composites for strain sensing. Compos Sci Tech, 2018, 167: 371–378
13 Choi W M, Song J, Khang D Y, et al. Biaxially stretchable "wavy" silicon nanomembranes. Nano Lett, 2007, 7: 1655–1663

14 Shang Y, He X, Li Y, et al. Super-stretchable spring-like carbon nanotube ropes. Adv Mater, 2012, 24: 2896–2900
15 Bowden N, Brittain S, Evans A G, et al. Spontaneous formation of ordered structures in thin films of metals supported on an elastomeric polymer. Nature, 1998, 393: 146–149
16 Lacour S P, Wagner S, Huang Z, et al. Stretchable gold conductors on elastomeric substrates. Appl Phys Lett, 2003, 82: 2404–2406
17 Gray D , Tien J, Chen C . High-conductivity elastomeric electronics. Adv Mater, 2004, 16: 393–397
18 Zhang Y, Guo J, Xu D, et al. Synthesis of ultralong copper nanowires for high-performance flexible transparent conductive electrodes: The effects of polyhydric alcohols. Langmuir, 2018, 34: 3884–3893
19 Liu N, Chortos A, Lei T, et al. Ultratransparent and stretchable graphene electrodes. Sci Adv, 2017, 3: e1700159
20 Tai Y L, Yang Z G. Flexible, transparent, thickness-controllable SWCNT/PEDOT:PSS hybrid films based on coffee-ring lithography for functional noncontact sensing device. Langmuir, 2015, 31: 13257–13264
21 Lee P, Lee J, Lee H, et al. Highly stretchable and highly conductive metal electrode by very long metal nanowire percolation network. Adv Mater, 2012, 24: 3326–3332
22 Zhang L Y, Wang J, Wei L M, et al. Synthesis of ni nanowires via a hydrazine reduction route in aqueous ethanol solutions assisted by external magnetic fields. Nano-Micro Lett, 2009, 1: 49–52
23 Xu C, Li Z, Yang C, et al. An ultralong, highly oriented nickel-nanowire-array electrode scaffold for high-performance compressible pseudocapacitors. Adv Mater, 2016, 28: 4105–4110
24 Liu H S, Pan B C, Liou G S. Highly transparent AgNW/PDMS stretchable electrodes for elastomeric electrochromic devices. Nanoscale, 2017, 9: 2633–2639
25 Shin M K, Oh J, Lima M, et al. Elastomeric conductive composites based on carbon nanotube forests. Adv Mater, 2010, 22: 2663–2667